Phase Transitions in $RbTiOPO_4$ Doped with Niobium

J. J. Carvajal, R. Solé, Jna. Gavaldà, J. Massons, F. Díaz, and M. Aguiló*

Laboratori de Física i Cristal·lografia de Materials, Universitat Rovira i Virgili, 43005 Tarragona, Spain

Received February 24, 2003. Revised Manuscript Received April 10, 2003

We used X-ray powder diffraction and differential thermal analysis (DTA) to study the effects of temperature on the cell parameters and phase transitions in $RbTi_{1-x}Nb_xOPO_4$ ($x = 0-0.9$) crystals. The linear thermal expansion coefficients were calculated from the results of X-ray diffraction. We determined their Curie temperature (T_c) by the change in the slope of the evolution of the *c* parameter of the crystals with the temperature, which is a function of the Nb content in the crystals. The transition temperature from RTP orthorhombic to $RbTiPO_5$ cubic phase and the decomposition temperature of this cubic phase, which are also functions of the Nb concentration in the crystals, were determined by DTA and X-ray diffraction. Finally, we also studied how the cell parameters of the RTP phase changed as the concentration of Nb in the crystals was increased at room temperature.

Introduction

Rubidium titanyl phosphate, $RbTiOPO_4$ (RTP), is isostructural with $KTiOPO_4$ (KTP). This family of compounds is attractive because of their excellent nonlinear optical properties.[1,2] RTP crystallizes, below its Curie temperature and at atmospheric pressure, in the noncentrosymmetric $Pna2_1$ space group with the lattice parameters $a = 12.974(2)$, $b = 6.494(3)$, and $c = 10.564(6)$ Å.[3]

At high temperature, the KTP and RTP structures show a reversible ferroelectric-to-paraelectric phase transition, with a Curie temperature (T_c) in the case of RTP ranging from 1058 to 1102 K.[4−7] After this second-order displacive phase transition, the crystal structure belongs to the centrosymmetric space group *Pnan*.[8]

A phase transition to a cubic phase (called decomposition in the literature) is observed for RTP at 1374 K.[9] This cubic phase, with the stoichiometry $RbTiPO_5$, crystallizes in the space group of symmetry $Fd\bar{3}m$, similarly to $CsTiPO_5$.[10] It seems that this cubic phase is stabilized by valence compensation when Nb^{5+} substitutes for the pair Ti^{4+}/Cs^+ in $CsTiAsO_5$.[11] In the literature, however, 1343 K was reported as the temperature of incongruent melting of RTP.[5,7] There is therefore an incongruity in the results in the literature regarding the decomposition of RTP at high temperature.

We have already studied rare earth (RE^{3+}) doping of KTP in previous papers.[12,13] The RE^{3+} distribution coefficients were very low, although codoping with Nb^{5+} enhanced the distribution coefficients of RE^{3+}.[11−13] However, Nb^{5+} is incorporated into the crystals and affects both the morphology and the physical properties of the materials.[12−15]

Interest in these crystals as laser materials makes it important to determine their linear thermal expansion coefficients and, thus, their thermal behavior. As is well-known, an important part of the pump power can be converted into heat inside the laser material during operation, so studying thermal effects on the solid-state laser materials is crucial in the design of solid-state laser devices.

In this paper, we determined the linear thermal expansion coefficients of RTP and RTP/Nb crystals and discuss their phase transitions with temperature. We show the different phase transitions of these crystals with temperature, and to make progress in the characterization of this host for RE^{3+}doping, we clarify the problems we found in the literature regarding the decomposition of RTP.

Experimental Procedures

Crystal Growth. $RbTi_{1-x}Nb_xOPO_4$ crystals with $x = 0-0.09$ were obtained from high-temperature solutions as described

* Corresponding author. E-mail: aguilo@quimica.urv.es.

(1) Masse, R.; Grenier, J. C. *Bull. Soc. Fr. Minéral. Cristallogr.* **1971**, *94*, 437.
(2) Hagerman, M. E.; Poeppelmeier, K. R. *Chem. Mater.* **1995**, *7*, 602.
(3) Thomas, P. A.; Mayo, S. C.; Watts, B. E. *Acta Crystallogr.* **1992**, *B48*, 401.
(4) Yanovskii, V. K.; Voronkova, V. I. *Phys. Status Solidi A* **1980**, *93*, 665.
(5) Cheng, L. K.; Bierlein, J. D.; Ballman, A. A. *J. Cryst. Growth* **1991**, *110*, 697.
(6) Wang, J. Y.; Liu, Y. G.; Wei, J. Q.; Shi, L. P.; Wang, M. *Z. Kristallogr.* **1990**, *191*, 231.
(7) Marnier, G.; Boulanger, B.; Ménaert, B. *J. Phys.: Condens. Matter.* **1989**, *1*, 5509.
(8) Harrison, W. T. A.; Gier, T. E.; Stucky, G. D.; Schultz, A. J. *Mater. Res. Bull.* **1995**, *30*, 1341.
(9) Cheng, L. K.; McCarron, E. M.; Calabrese, J.; Bierlein, J. D.; Ballman, A. A. *J. Cryst. Growth* **1993**, *132*, 280.
(10) Kunz, M.; Dinnebier, R.; Cheng, L. K.; McCarron, E. M.; Cox, D. E.; Parise, J. B.; Gehrke, M.; Calabrese, J.; Stephens, P. W.; Vogt, T.; Papoular, R. *J. Solid State Chem.* **1995**, *120*, 299.
(11) Solé, R.; Nikolov, V.; Koseva, I.; Peshev, P.; Ruiz, X.; Zaldo, C.; Martín, M. J.; Aguiló, M.; Díaz, F. *Chem. Mater.* **1997**, *9*, 2745.
(12) Carvajal, J. J.; Nikolov, V.; Solé, R.; Gavaldà, Jna.; Massons, J.; Rico, M.; Zaldo, C.; Aguiló, M.; Díaz, F. *Chem. Mater.* **2000**, *12*, 3171.
(13) Carvajal, J. J.; Nikolov, V.; Solé, R.; Gavaldà, Jna.; Massons, J.; Aguiló, M.; Díaz, F. *Chem. Mater.* **2002**, *14*, 3136.
(14) Carvajal, J. J.; Solé, R.; Gavaldà, Jna.; Massons, J.; Rico, M.; Zaldo, C.; Aguiló, M.; Díaz, F. *J. Alloys Compd.* **2001**, *323−324*, 231.
(15) Carvajal, J. J.; Solé, R.; Gavaldà, Jna.; Massons, J.; Aguiló, M.; Díaz, F. *Cryst. Growth Des.* **2001**, *1*, 479.

10.1021/cm0340936 CCC: $25.00
Published on Web 00/00/0000 PAGE EST: 6.2

previously.[12] The temperature of the homogeneous solution was lowered in ~10 K steps every 30 min until crystals appeared on a platinum wire immersed in the solution. The temperature was then decreased at a rate of 0.5−1 K/h for about 20 K so that the crystals could grow slowly and with high quality. We analyzed the chemical composition of the crystals by electron probe microanalyses with wavelength-dispersion spectroscopy (EPMA-WDS) in a CAMECA SX-50 instrument as explained elsewhere.[13]

X-ray Powder Diffraction. We used Cu Kα X-ray radiation to collect diffraction patterns of $RbTi_{1-x}Nb_xOPO_4$ crystals, $x = 0-0.09$, on a Siemens D5000 powder diffractometer in a $\theta-\theta$ goniometer using Bragg−Brentano parafocusing geometry with an Anton-Paar HTK10 platinum ribbon heating stage. The goniometer was fitted with a diffracted-beam curved graphite monochromator and a scintillation counter as the detector. We performed three kinds of experiments: First, we determined how the cell parameters of $RbTi_{1-x}Nb_xOPO_4$ crystals, $x = 0-0.09$, evolved as the concentration of Nb in the crystals increased. To do this, we determined the X-ray powder diffraction data at $2\theta = 10-70°$, ss (step scan) = 0.02°, and st (scan time) = 16 s at room temperature. Second, we took another series of measurements to study how the cell parameters and the thermal expansion coefficients of $RbTi_{1-x}Nb_xOPO_4$ crystals with $x = 0$, 0.05, and 0.09 evolved as the temperature was increased. In this case, the powder diffraction data were obtained at $2\theta = 10-70°$, ss = 0.03°, and st = 5 s in the 298−1198 K temperature range. The temperature was increased at a rate of 5 $K{\cdot}s^{-1}$. The sample was left for 1800 s at the measuring temperature to stabilize the equipment and the sample. Third, we took a series of measurements to study the evolution and phase transition of $RbTi_{1-x}Nb_xOPO_4$, $x = 0$ and 0.09, as the temperature was increased. In this case we used a Braun position-sensitive detector (PSD). The powder diffraction data were obtained at $2\theta = 10-70°$, and the measuring time per degree was 10 s in the 973−1373 K range in the heating and cooling cycles. Patterns were registered every 50 K, and a delay of 200 s was introduced before each measurement. We increased the temperature at a rate of 5 $K{\cdot}s^{-1}$ between room temperature and 973 K and at a rate of 1 $K{\cdot}s^{-1}$ between 973 and 1323 K. To study the transition from the orthorhombic phase to the cubic phase, we applied a rate of 0.1 $K{\cdot}s^{-1}$ between 1323 and 1373 K in the heating cycle and between and 1373 and 1273 K in the cooling cycle. We then also decreased the temperature at a rate of 1 $K{\cdot}s^{-1}$ between 1273 and 973 K and at a rate of 5 $K{\cdot}s^{-1}$ from 973 K to room temperature.

Data Refinement. We refined the crystal cell parameters with the FULLPROF program[16] and the Rietveld method.[17] We used the coordinates of the atoms obtained by Thomas et al.[2] in the case of RTP and the coordinates calculated previously by us[18] in the case of RTP/Nb crystals as the starting model for the calculations and selected a Pearson VII function to describe individual line profiles.

To determine how the cell parameters and cell volume of $RbTi_{1-x}Nb_xOPO_4$ ($x = 0-0.09$) crystals evolved as the concentration of Nb was increased at room temperature, the final Rietveld refinement included the following parameters: the zero point, the scale factor, one or three background coefficients, the three cell parameters, three half-width parameters, and one profile shape parameter. To determine how the cell parameters and cell volume of $RbTi_{1-x}Nb_xOPO_4$ ($x = 0$, 0.05, and 0.09) crystals evolved as the temperature increased, the final Rietveld refinement included the following parameters: the scale factor; one, two, or three background coefficients; the three cell parameters; one half-width parameter; one profile shape parameter; and one preferential orientation parameter. The zero point was refined only at room temperature. It was not necessary at the remaining temperature because the sample was always the same and was not moved when the temperature was increased, so this parameter was fixed. Furthermore, refining on the zero point did not introduce any improvement in the fitting results. In this case, peaks of Pt were observed because the sample was placed on a plate of this material. We then also refined the Pt phase. In this case, the final Rietveld refinement included the following parameters for the Pt phase: the scale factor, the cell parameter, and one preferential orientation parameter.

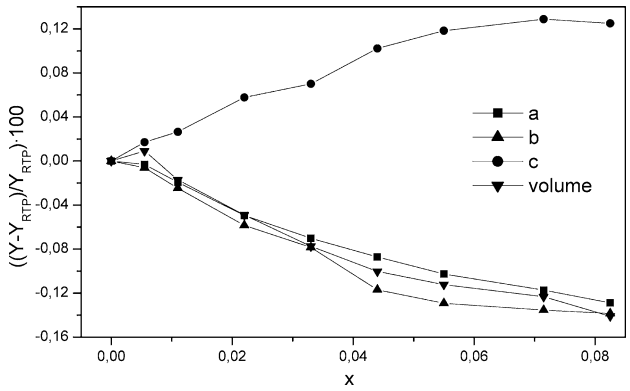

Figure 1. Evolution of the cell parameters and cell volume of the $RbTi_{1-x}Nb_xOPO_4$ crystals as a function of the concentration of niobium ($Y = a$, b, c, or volume).

Differential Thermal Analysis (DTA) Measurements. We also studied, by differential thermal analysis (DTA) using a TA Instruments Simultaneous Differential Techniques Instrument SDT 2960, the phase transitions of RTP and RTP/Nb crystals at high temperature before the decomposition of the RTP material. The experiments were carried out in Pt pans using calcined Al_2O_3 as the reference material. To obtain information about the reversibility of this phase transition, both the sample (weighing around 30 mg) and the reference material (with a weight similar to that of the sample) were heated at 10 K/min in the 298−1573 K range in the heating and cooling cycles. We used Ar as the purge gas at a flow rate of 90 cm^3/min. The storage rate of data was always 0.5 s per data point.

Results and Discussion

Variation of the Lattice Parameters of $RbTi_{1-x}Nb_xOPO_4$ with the Concentration of Nb. Figure 1 shows a plot of the evolution of the lattice parameters and the volume of $RbTi_{1-x}Nb_xOPO_4$ crystals as functions of the concentration of Nb^{5+} in the crystal. We represent the increase or decrease in the different parameters with respect to the same parameter of pure RTP in the following way: $[(Y - Y_{RTP})/Y_{RTP}] \times 100$, where Y is the value of a parameter in the crystal analyzed and Y_{RTP} is the same parameter for the pure RTP crystal. The a and b parameters decrease whereas c increases as the concentration of Nb increases. The cell volume decreases as the concentration of Nb in the crystal increases. These changes in the lattice cell are different from those reported for KTP doped with Nb in the literature,[19] where parameter a essentially did not change for the doping level studied and parameters b and c increased as the Nb^{5+} doping increased.

A self-compensation of the excess of electrical charge of the crystals by the substitution of Ti^{4+} by Nb^{5+} by the mechanism of creating Rb^+ vacancies was observed.[18] This could be why substituting Ti^{4+} with an

(16) Rodríguez-Carvajal, J. *Physica B* **1993**, *192*, 55.
(17) Young, R. A. *The Rietveld Method*; Oxford Science Publications, International Union of Crystallography: Oxford, U.K., 1995.
(18) Carvajal, J. J.; García-Muñoz, J. L.; Solé, R.; Gavaldà, Jna.; Massons, J.; Solans, X.; Díaz, F.; Aguiló, M. *Chem. Mater.*, manuscript submitted.
(19) Cheng, L. T.; Cheng, L. K.; Harlow, R. L.; Bierlein, J. D. *Appl. Phys. Lett.* **1994**, *64*, 155.

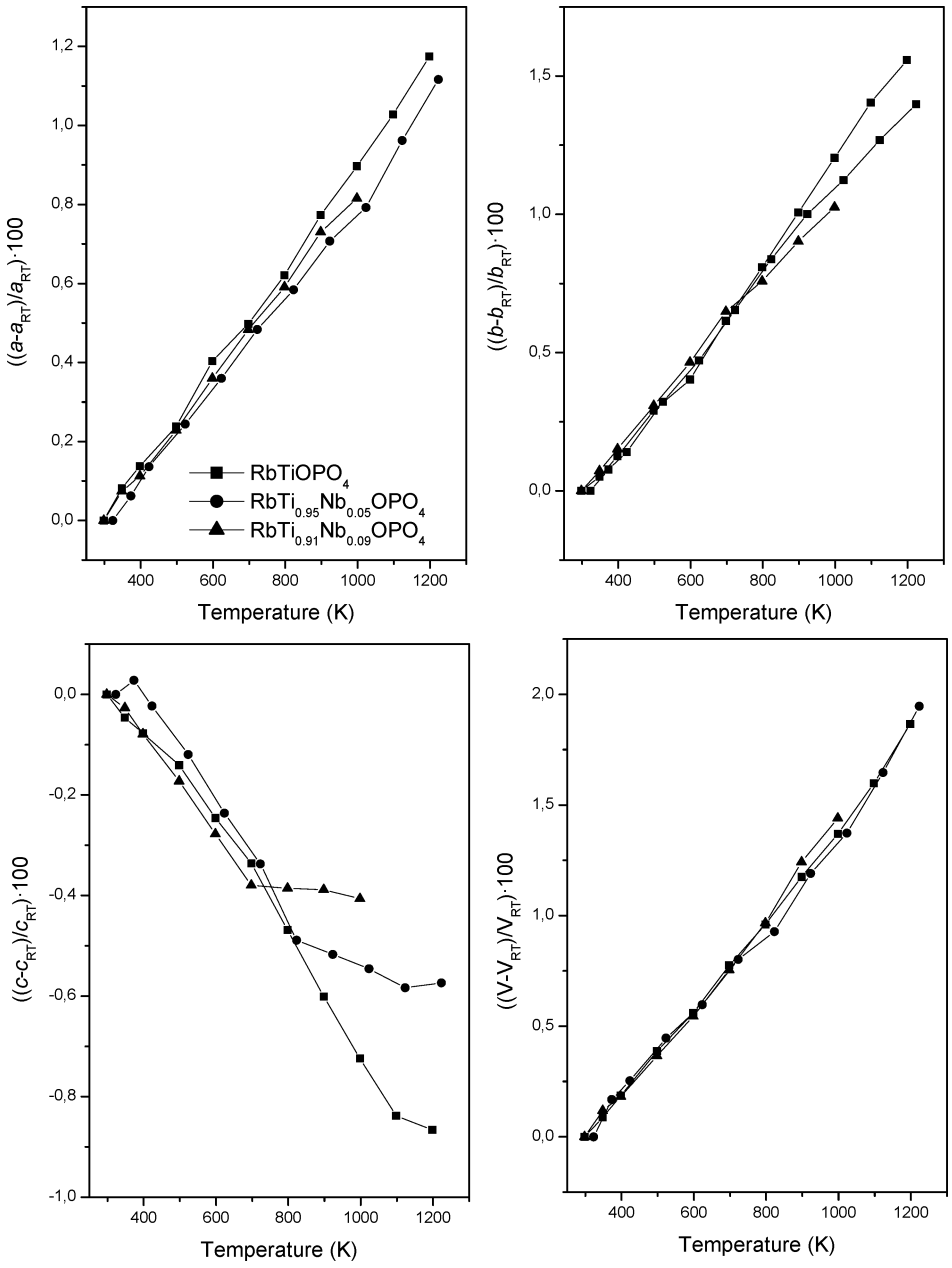

Figure 2. Evolution of the cell parameters and cell volume of the $RbTi_{1-x}Nb_xOPO_4$ ($x = 0$, 0.05, and 0.09) crystals with temperature.

ion with a larger ionic radius (Ti^{4+} has an ionic radius of 0.605 Å in an octahedral environment, and Nb^{5+} has an ionic radius of 0.64 Å in the same environment[20]) did not, as we should expect, increase the three cell parameters of the structure. The vacancies of Rb^+ can compensate both the excess of electrical charge in the crystal and the change in the cell parameters. However, we were not able to determine the loss in Rb^+ by EPMA analyses, and for that reason, we write the chemical formula of RTP crystals doped with Nb as $RbTi_{1-x}Nb_xOPO_4$.

Thermal Expansion Coefficients. Figure 2 shows a plot of the evolution of the lattice parameters and volume of the $RbTi_{1-x}Nb_xOPO_4$ ($x = 0$, 0.05 and 0.09) crystals as functions of temperature. Whereas the volume and parameters *a* and *b* increase as the temperature increases, *c* decreases. This behavior has been observed in KTP[21] and RTP.[22] The most important feature of the evolution of the cell parameters with temperature is the dramatic change in the slope of the evolution of the *c* parameter. This change also depended on the concentration of Nb, as occurred at lower temperatures as the concentration of Nb increased.

We attributed this change to the transition from the ferroelectric phase to the paraelectric phase by analogy with the work of Yanovskii et al.[23] on KTP/Nb. The Nb in the crystal affected this transition, and when the concentration of Nb increased, the Curie temperature (T_c) decreased. This is very important, because the paraelectric phase loses the nonlinear optical properties

(20) Shannon, R. D. *Acta Crystallogr.* **1976**, *A32*, 751.

(21) Delarue, P.; Lecomte, C.; Jannin, M.; Marnier, G.; Ménaert, B. *J. Phys.: Condens. Matter.* **1999**, *11*, 4123.

(22) Delarue, P.; Lecomte, C.; Jannin, M.; Marnier, G.; Menaert, B. *Phys. Rev. B* **1998**, *58*, 5287.

(23) Yanovskii, V. K.; Voronkova, V. I.; Losevskaya, T. Y.; Stefanovich, T. Y.; Ivanov, S. A.; Simonov, V. I.; Sorokina, N. I. *Crystallogr. Rep.* **2002**, *47*, S199.

Table 1. Linear Expansion Coefficients α_{ij} (10^{-6}, K^{-1}) of $RbTi_{1-x}Nb_xOPO_4$ Crystals

x	α_{11}	α_{22}	α_{33}
0	12.7(2)	17.7(5)	−10.5(4)
0.05	11.7(2)	16.7(3)	−10.2(8)
0.09	11.9(3)	16.1(3)	−9.7(3)

of the ferroelectric phase. This way of visualizing the phase transition, in this family of compounds, from the ferroelectric phase to the paraelectric phase over the evolution of the *c* parameter with the temperature has not yet been described in the literature.

This material is interesting as a possible laser medium; thus, because a significant part of the power pump is converted into heat inside the laser material during operation, it might be subjected to temperatures above room temperature. Therefore, its linear thermal expansion coefficients should be known, to predict how it behaves when the temperature increases. The linear thermal expansion coefficients in a given crystallographic direction, assumed to be independent of temperature are represented by $\alpha = (\Delta L/\Delta T)/L$, where L is the initial parameter at room temperature and ΔL is the change in this parameter as the temperature changes by ΔT. These thermal expansion coefficients were calculated from the slopes of the linear fittings of the relationship between $(\Delta L/L)$ and temperature in the different crystallographic directions. We used only the lattice parameters in the first linear range of the evolution of each parameter with temperature. Table 1 shows the thermal expansion coefficients for $RbTi_{1-x}Nb_xOPO_4$ crystals with $x = 0$, 0.05, and 0.09. The results for pure RTP agree well with those reported in the literature.[19] The RTP/Nb thermal expansion coefficients, given for the first time here, are slightly smaller than those for RTP (see Table 1); the thermal anisotropy is also lower, which implies less thermal stress in the crystal. It seems that the α_{11}, α_{22}, and α_{33} thermal-expansion coefficients decrease in absolute value as the concentration of Nb in the crystal increases.

Phase Transition Studies. A complete study of the phase transitions in RTP with temperature has not yet been published, and the results in the literature for the different phase transitions of this material are inconsistent. We have studied the phase transitions of $RbTi_{1-x}Nb_xOPO_4$ crystals with $x = 0$ and 0.09 with temperature by X-ray powder diffraction and DTA analyses. Table 2 shows the phases observed with the changes in temperature in the $RbTi_{1-x}Nb_xOPO_4$ ($x = 0$ and 0.09) crystals.

Figure 3a shows, for pure $RbTiOPO_4$ crystals, a detailed view of the evolution of the powder diffraction pattern with temperature. We can see that the RTP phase was present between room temperature and 1323 K as the temperature was increased. Above 1323 K, we detected two new compounds. We identified the first as the high-temperature cubic phase of RTP, with the spatial group of symmetry $Fd\bar{3}m$ and the stoichiometry of $RbTiPO_5$. We identified the second as the result of the decomposition of this cubic phase: Rb_2O and P_2O_5 evaporated, but the TiO_2 in the rutile phase remained in the solid state. Thermal hysteresis was detected in the phase transition from the orthorhombic phase to the cubic phase in RTP because, in the cooling cycle, the orthorhombic phase reappeared at 1173 K. From 1173 to 973 K, the intensity of the peaks in the cubic phase started to decrease. These intensities then remained constant, but the intensity of the peaks in the RTP phase increased over the same range of temperatures. However, $RbTiPO_5$ was detected thoughout the range of temperatures in the cooling cycle, although as a minority phase. An unusual aspect was also the increase in the intensity of the peaks in the rutile phase between 1373 and 1323 K in the cooling cycle. This was due either to better crystallization or to a larger amount of $RbTiPO_5$, despite the lower temperature. The intensity of the peaks in this phase then remained constant in all pattern files of the cooling cycle.

Table 2. Phase Transitions in $RbTiOPO_4$ and $RbTi_{0.91}Nb_{0.09}OPO_4$ with Temperature

temperature (K)	$RbTiOPO_4$	$RbTi_{0.91}Nb_{0.09}OPO_4$
973	RTP	RTP
1073	RTP	RTP
1173	RTP	RTP
1273	RTP	RTP $RbTiPO_5$
1323	RTP $RbTiPO_5$ TiO_2	RTP $RbTiPO_5$ TiO_2
1373	$RbTiPO_5$ TiO_2 (rutile)	$RbTiPO_5$ TiO_2 (rutile) NbO_2
1323	$RbTiPO_5$ TiO_2 (rutile)	$RbTiPO_5$ TiO_2 (rutile) NbO_2
1273	$RbTiPO_5$ TiO_2 (rutile)	$RbTiPO_5$ TiO_2 (rutile) NbO_2
1173	RTP $RbTiPO_5$ TiO_2 (rutile)	$RbTiPO_5$ TiO_2 (rutile) NbO_2
1073	RTP $RbTiPO_5$ TiO_2 (rutile)	$RbTiPO_5$ TiO_2 (rutile) NbO_2
973	RTP $RbTiPO_5$ TiO_2 (rutile)	$RbTiPO_5$ TiO_2 (rutile) NbO_2
room temperature	RTP $RbTiPO_5$ TiO_2 (rutile)	$RbTiPO_5$ TiO_2 (rutile) NbO_2

The phase transition of RTP from the ferroelectric phase ($Pna2_1$) to the paraelectric phase ($Pnan$), which could be followed by a change in the slope of the evolution of the *c* parameter with temperature, cannot be detected by analyzing the X-ray powder diffraction patterns of these phases, because all of the peaks that produced extinction with the change in symmetry from $Pna2_1$ to $Pnan$ have such low intensity that the existence or the extinction of these peaks cannot be concluded.

Figure 3b shows how the powder diffraction patterns of $RbTi_{0.91}Nb_{0.09}OPO_4$ evolved as the temperature was increased. If this figure iis described n terms of the phases appearing or disappearing as temperature increased, we can see that, between 973 and 1173 K, the orthorhombic RTP was the only phase present. Above 1173 K, the cubic $RbTiPO_5$ phase appeared. Unlike pure RTP, however, this phase coexisted with the RTP orthorhombic phase between 1173 and 1323 K. At 1173 K, the cubic phase did not show all of the expected peaks of the X-ray powder pattern, but above 1323 K, the intensity of the peaks appeared before increased and new peaks of this phase appeared. Above 1323 K, the orthorhombic RTP phase disappeared, and in addition

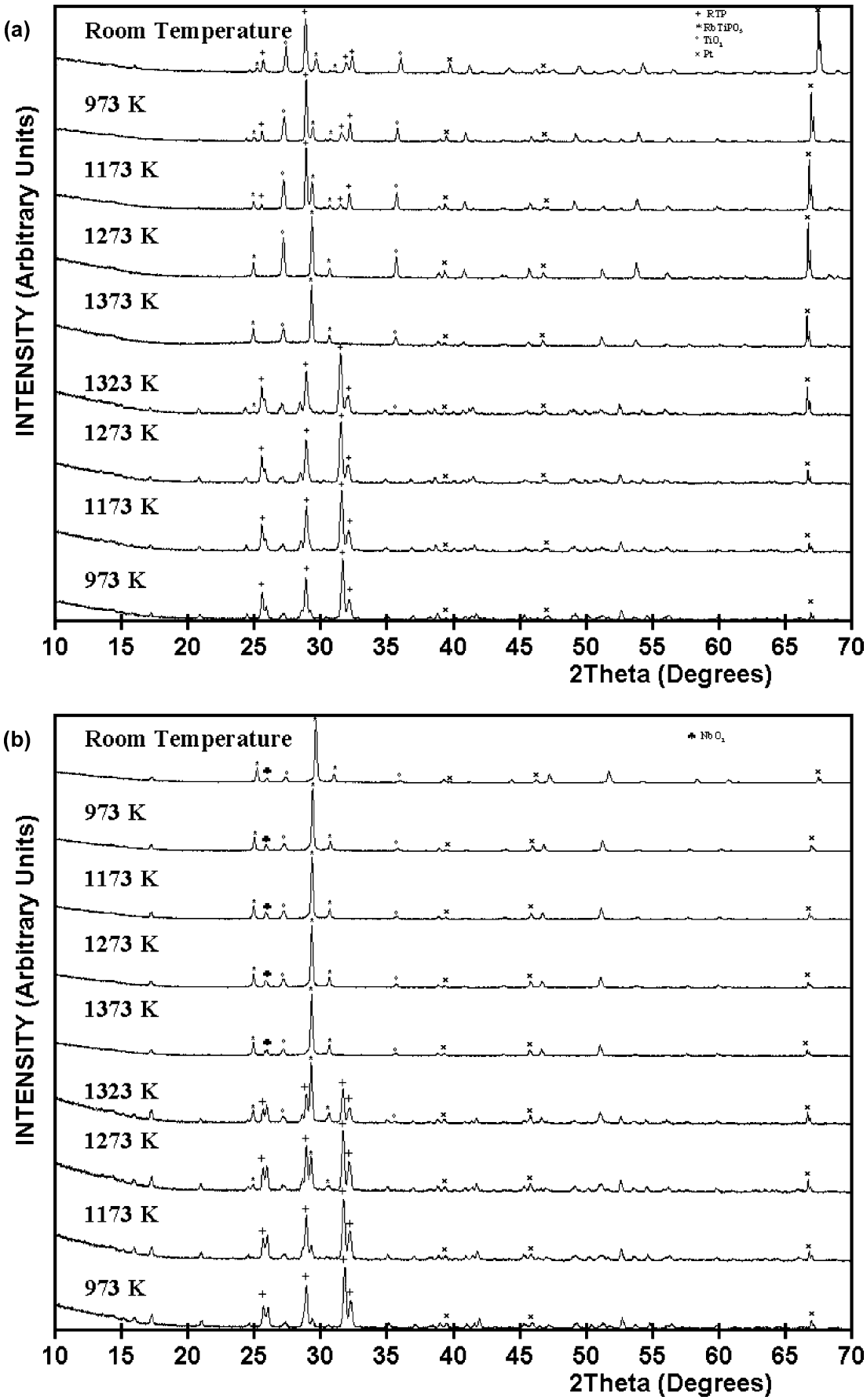

Figure 3. Selected X-ray powder patterns at different temperatures showing the phase transitions of (a) $RbTiOPO_4$ and (b) $RbTi_{0.91}Nb_{0.09}OPO_4$ crystals.

to the cubic $RbTiPO_5$ phase, TiO_2 (rutile) and NbO_2 phases appeared. In the cooling cycle, $RbTiPO_5$, rutile, and NbO_2 phases remained, and the orthorhombic RTP phase did not reappear. We can say, then, that unlike

Table 3. Phase Transition Temperatures in $RbTi_{1-x}Nb_xOPO_4$ (x = 0, 0.05, and 0.09) Crystals

	$RbTiOPO_4$	$RbTi_{0.95}Nb_{0.05}OPO_4$	$RbTi_{0.91}Nb_{0.09}OPO_4$
T_c ($Pna2_1 \rightarrow Pnan$)	1090−1198 K	823−923 K	698−798 K
$T_{o\rightarrow c}$ ($Pnan \rightarrow Fd\bar{3}m$)	1352 K	1345 K	1330 K
T_d (decomposition)	1414 K	1434 K	1463 K

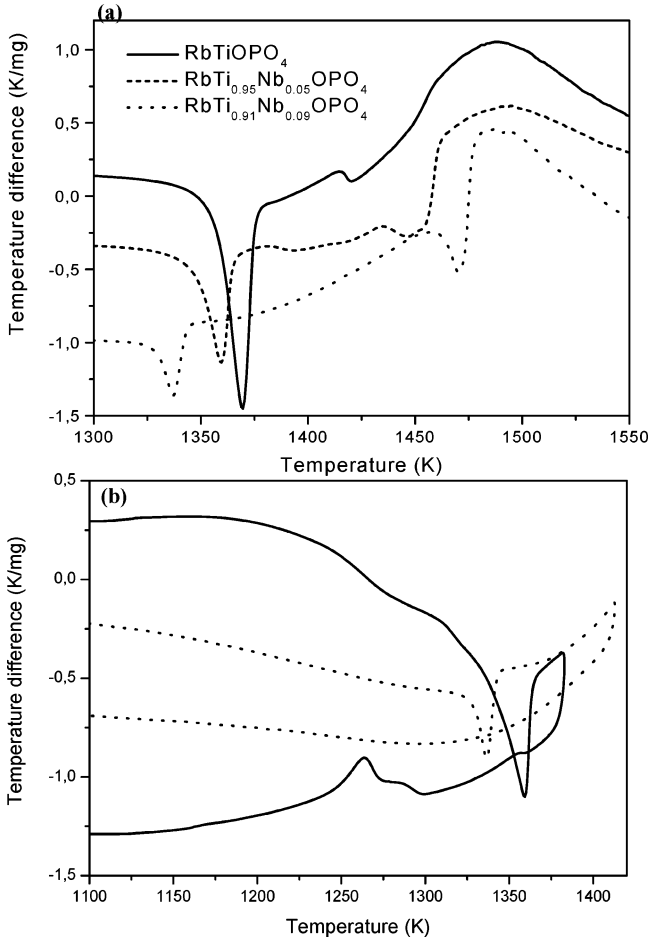

Figure 4. Differential thermal analysis (DTA) thermograms of (a) $RbTi_{1-x}Nb_xOPO_4$ (x = 0, 0.05, and 0.09) crystals between 1300 and 1550 K and (b) $RbTi_{1-x}Nb_xOPO_4$ (x = 0 and 0.09) crystals in the heating and cooling processes.

with pure RTP, the phase transition in this case was irreversible. This assumption was corroborated by DTA measurements (see Figure 4).

Figure 4a shows the results of DTA analyses of $RbTi_{1-x}Nb_xOPO_4$ crystals (x = 0, 0.05, and 0.09). We observed only the transition from the orthorhombic RTP phase to the cubic $RbTiPO_5$ phase and the decomposition of this latter phase. There was a significant loss in weight that coincided with the second peak of the thermogram, the one that we attributed to the decomposition of the cubic phase. As can also be seen in this figure, the temperature of the transition from the orthorhombic phase to the cubic phase, as well as the temperature of decomposition of this latter phase, is a function of the concentration of Nb in the crystals. As the concentration of Nb in the crystals increased, the temperature of the transition from the orthorhombic phase to the cubic phase decreased, and the temperature of decomposition increased. This might be due to the stability of the cubic $RbTiPO_5$ phase induced by the Nb. If the cubic phase is more stable because Nb is incorporated into the crystals, the activation energy needed to generate this new cubic phase from the orthorhombic phase might be lower than that required when there is no Nb in the crystal. Consequently, the temperature of the transition between the orthorhombic RTP phase and cubic $RbTiPO_5$ phase decreases as the concentration of Nb in the crystal increases. This was confirmed by the lower intensity of the phase transition peak as the concentration of Nb in the samples increased, since the measurements were always made with similar sample weights that cannot explain these changes in intensity. This transition from the orthorhombic phase to the cubic phase is reversible (in the sense that we mentioned earlier) for pure RTP crystals and irreversible for RTP/Nb crystals (see Figure 4b). The same stabilization of the cubic phase might be responsible for the higher decomposition temperature of the cubic phase. As this cubic phase was more stable, more energy was needed to decompose it, so the decomposition temperature increased. This was also confirmed by the greater intensity of the peak of decomposition as the concentration of Nb increased (see Figure 4a). These results show that, when Nb^{5+} substitutes for the pair Ti^{4+}/Rb^+ in RTP, the $RbTiPO_5$ cubic phase is stabilized by valence compensation.

Table 3 shows the phase transition temperatures in this study for $RbTi_{1-x}Nb_xOPO_4$ crystals with x = 0, 0.05, and 0.09. The temperatures corresponding to the transitions from the orthorhombic Pnan phase to the cubic $Fd\bar{3}m$ phase and the later decomposition of this cubic phase were the onset temperatures determined from DTA. Using these results, we suggest that the chemical reaction as the is temperature increased, depending on whether Nb^{5+} is present in the crystals, is

$$RbTiOPO_4\ (\text{ferroelectric},\ Pna2_1) \overset{T_c}{\longleftrightarrow} RbTiOPO_4\ (\text{paraelectric},\ Pnan) \overset{T_{o\rightarrow c}}{\longleftrightarrow} RbTiPO_5\ (\text{cubic},\ Fd\bar{3}m) \xrightarrow{T_d} Rb_2O\ (g) + P_2O_5\ (g) + TiO_2\ (\text{rutile})$$

$$RbTi_{1-x}Nb_xOPO_4\ (\text{ferroelectric},\ Pna2_1) \overset{T_c}{\longleftrightarrow} RbTi_{1-x}Nb_xOPO_4\ (\text{paraelectric},\ Pnan) \overset{T_{o\rightarrow c}}{\longrightarrow} RbTiPO_5\ (\text{cubic},\ Fd\bar{3}m) \xrightarrow{T_d} Rb_2O\ (g) + P_2O_5(g) + TiO_2\ (\text{rutile}) + NbO_2$$

where T_c is the Curie temperature, $T_{o\rightarrow c}$ is the phase transition temperature for the transition from the orthorhombic RTP phase to the cubic $RbTiPO_5$ phase, and T_d is the temperature of decomposition.

Conclusions

We have studied all of the phase transitions that take place in RTP as the temperature increases. We also studied RTP crystals doped with Nb, which provided us with more information about how these phase transi-

tions are affected when Nb is present in the crystals. The transition from the orthorhombic $Pna2_1$ phase to the *Pnan* phase, as well as the transition from the orthorhombic RTP phase to the cubic $RbTiPO_5$ phase, occurred at lower temperature as the concentration of Nb in the crystal increased. Also, the decomposition temperature of the cubic $RbTiPO_5$ phase increased, which indicated that substituting the Ti^{4+}/Rb^{+} pair with Nb^{5+} stabilized the cubic $RbTiPO_5$ phase. The transition temperature from the ferroelectric phase to the paraelectric phase was obtained by the change in the slope of the evolution of the *c* parameter of the structure with temperature. This method was not available in the literature until now.

Acknowledgment. The authors are grateful to CIRIT for supporting this work under Project 2001SGR317 and to CICyT for supporting this work under Projects MAT2002-4603-C05-03 and FIT-070000-2002-461. We also thank the Serveis Cientifico-Tècnics of the Universitat de Barcelona for kindly supplying helpful measurements on EPMA. J.J.C. also acknowledges the grant he received from the Catalan Government (2000FI 00633 URV APTIND).

CM0340936

Initial Page Papers